

Impedance Studies on $\text{Ca}_{0.5}\text{Sr}_{0.5}\text{Cu}_3\text{Ti}_4\text{O}_{12}$ Ceramic Oxide

Mazni Mustafa, W. Mohamad Daud W. Yusoff*, Zainal Abidin Talib,
Abdul Halim Shaari and Walter Charles Primus

*Department of Physics, Faculty of Science, Universiti Putra Malaysia,
43400 UPM, Serdang, Selangor, Malaysia*

**E-mail: wmdaud@science.upm.edu.my*

ABSTRACT

$\text{Ca}_{0.5}\text{Sr}_{0.5}\text{Cu}_3\text{Ti}_4\text{O}_{12}$ (CSCTO) ceramic oxide was prepared using solid state reaction technique. Impedance measurement was done using High Dielectric Resolution Analyzer (Novocontrol Novotherm) from 30°C to 250 °C, in the frequency range of 10^2 to 10^6 Hz. X-ray diffraction pattern showed a single phase with a cubic structure. In the complex impedance plot, three semi-circles were observed; these represented the grain, grain boundary and electrode effect responses. The semi-circles were fitted using a series network of three parallel RC circuits. The resistance was found to increase with the decreasing temperature. The activation energies, E_a , obtained from the Arrhenius plots of CSCTO, were 0.31 eV and 0.73 eV for grain and grain boundary conductivity, respectively. The value of the grain energy was revealed as smaller than the grain boundary energy, due to the semi-conducting grain and the insulating grain boundary characteristic (Sinclair *et al.*, 2002).

Keywords: CCTO, impedance, grain boundary, Arrhenius

INTRODUCTION

The $\text{ACu}_3\text{Ti}_4\text{O}_{12}$ family of compounds has been known since 1967, and most exceptional behaviour was exhibited by the $\text{CaCu}_3\text{Ti}_4\text{O}_{12}$ (CCTO) ceramics. The CCTO was first synthesized in 1979, and has a cubic perovskite structure with space group $Im-3$ (Bochu *et al.*, 1979). The CCTO shows a giant dielectric response and has an extremely high value of dielectric constant ϵ' , at 1 kHz of about 10,000 (Subramanian *et al.*, 2000). Based on the impedance spectroscopy (IS), a high permittivity is associated to an “extrinsic” effect, due to an internal barrier layer capacitance (IBLC) effect, where insulating surfaces or grain boundaries are formed on the semi-conducting grains during the processing of the CCTO ceramics (Guillemet-Fritsch *et al.*, 2006). It was reported that most compositions of $\text{A}_{2/3}\text{Cu}_3\text{Ti}_4\text{O}_{12}$ (A = trivalent rare earth) showed dielectric constants above 1000 at 100 kHz. Those of the compositions $\text{ACu}_3\text{Ti}_4\text{O}_{12}$ (A = Ca, Sr or Ba) also showed dielectric constants above 1000, except for $\text{BaCu}_3\text{Ti}_4\text{O}_{12}$, which revealed a value below 1000 (Ohwa *et al.*, 2004). In this article, the microstructures of both CCTO and strontium substituted CCTO (CSCTO) are reported. The impedance properties of the CSCTO were also studied at different temperatures.

THEORY

The frequency dependent properties of a material can be described in four possible complex formalisms; these are complex permittivity ($\epsilon^* = \epsilon' - i\epsilon''$), complex impedance ($Z^* = Z' - iZ''$),

Received: 11 January 2008

Accepted: 8 April 2008

*Corresponding Author

complex admittance ($Y^* = Y' + iY''$), and complex electric modulus ($M^* = M' + iM''$). The above formalisms are interrelated as:

$$\varepsilon^* = \frac{1}{i\omega Z^* C_o} = \frac{Y^*}{i\omega C_o} = \frac{1}{M^*} \quad (1)$$

Where, $C_o = \varepsilon_o A/d$, A is the area, d is the thickness of the sample, ω is the angular frequency ($2\pi f$) and $\varepsilon_o = 8.854 \times 10^{-14} \text{ Fcm}^{-1}$ is the permittivity of free space.

The complex impedance plot was fitted using the universal capacitor $C^* = B (i\omega)^{-n}$, where B is a constant, n lies in the range $0 < n < 1$, and R is the resistance. The resistivity ρ was calculated using $\rho = RA/d$, where R is the resistance value from the fitting results, A is the area and d is the distance. The conductivity σ was calculated using the resistivity data by equation $\sigma = 1/\rho$. The conductivity σ follows the Arrhenius law and can be described by the following expression:

$$\sigma = \sigma_o \exp (-E_a/kT) \quad (2)$$

where E_a is the activation energy, and k is the Boltzmann's constant.

MATERIALS AND METHODS

$\text{CaCu}_3\text{Ti}_4\text{O}_{12}$ (CCTO) and strontium substituted CCTO (CSCTO) ceramics were prepared, using solid state reaction technique, from the raw materials such as calcium carbonate (CaCO_3), strontium carbonate (SrCO_3), titanium dioxide (TiO_2) and copper (II) oxide (CuO). These materials were weighed according to the stoichiometric ratios and were ground for 3 hours. The mixed powders were calcined at 900 °C for 10 hours. The calcined powder was reground for 2 hours to improve its homogeneity, before sintering in air at 1050 °C for 24 hours in powder and pellet forms. The XRD was done on the sintered powder to monitor the phase evolution using Philips (Model PW3040). After that, these sintered pellets were polished to achieve flat and parallel surfaces and were sputtered with silver as electrode, using the RF Magnetron Sputtering. The impedance measurement was done from 30 °C to 250 °C, in the frequency range of 10^2 to 10^6 Hz, using a High Dielectric Resolution Analyzer (Novocontrol Novotherm).

RESULTS AND DISCUSSION

The XRD patterns for both CCTO and CSCTO are shown in *Fig. 1*. The patterns show single phases for both samples, while cubic structure with calculated lattice parameter $a = 7.4041 \text{ \AA}$ was compared to 7.3590 \AA (Jha *et al.*, 2003). *Fig. 2* shows the SEM images of the surfaces of the CCTO and CSCTO. The morphology shows grain and grain boundary for both the samples. The grain size for the CSCTO is much larger than the CCTO grain size.

The complex impedance provided the grain and the grain boundary effects, as well as the capacitive, C and resistive, R element of the samples. Using the fitting approach of the universal capacitor, $C^* = B (i\omega)^{-n}$, the grain and grain boundary effects could be separated due to the existence of the semi-circles.

Fig. 3(a) shows complex impedance plots for the CSCTO at selected temperatures of 190 °C and 230 °C. The graphs show three semi-circles, as illustrated in *Fig. 3(b)*. The high frequency semi-circle is attributed to the grain properties, while the second semi-circle is

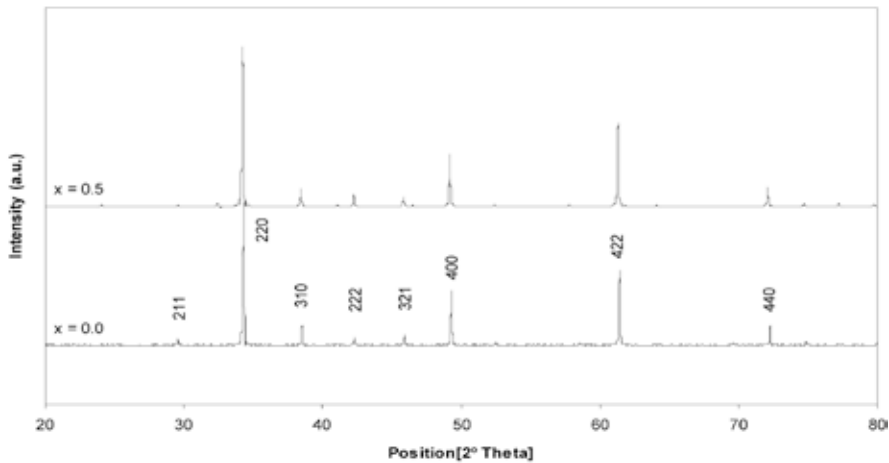
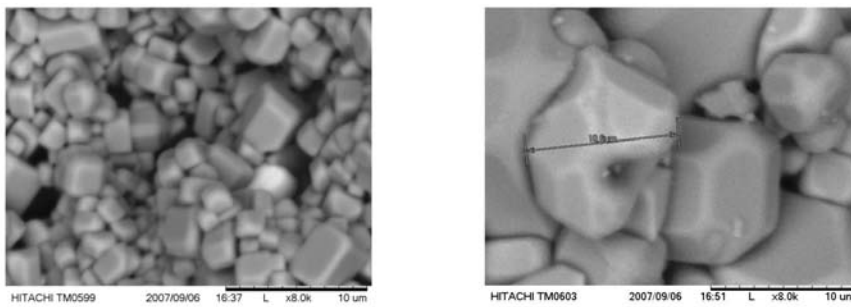


Fig. 1: X-ray diffraction patterns of both CCTO and CSCTO



(a)

(b)

Fig. 2: Electron micrographs for (a) CCTO, and (b) CSCTO consisting of grain and grain boundary

assigned to the grain boundary properties. The third semi-circle, at the low frequency, is due to the electrode effects. The presence of the three semi-circles are modelled as an equivalent electrical circuit, which comprises a combination of the series network of three parallel RC circuits, as depicted in Fig. 4. The fitting parameters for the CSCTO are listed in Table 1. The grain resistance (R_g) and grain boundary resistance (R_{gb}) were obtained from the intercept of the semi-circles on the real axis, Z' . It could be obviously observed that the resistance was increased when the temperature decreased from 230 °C to 70 °C. The frequency peak ω_p was also found to increase as the temperature increased. The semi-circles were inclined at an angle of $n\pi/2$, where the n values for the grain region were increased from 0.98 to 1 as the temperature decreased. The n values for the grain boundary region were in the range of 0.70 to 0.80, between 70 °C to 230 °C. If $n = 1$, the universal capacitor would give an ideal capacitor, where $C^* = C$. As for the grain region, a pure C was observed, while at the grain boundary region, the universal capacitor gave both capacitance and resistance.

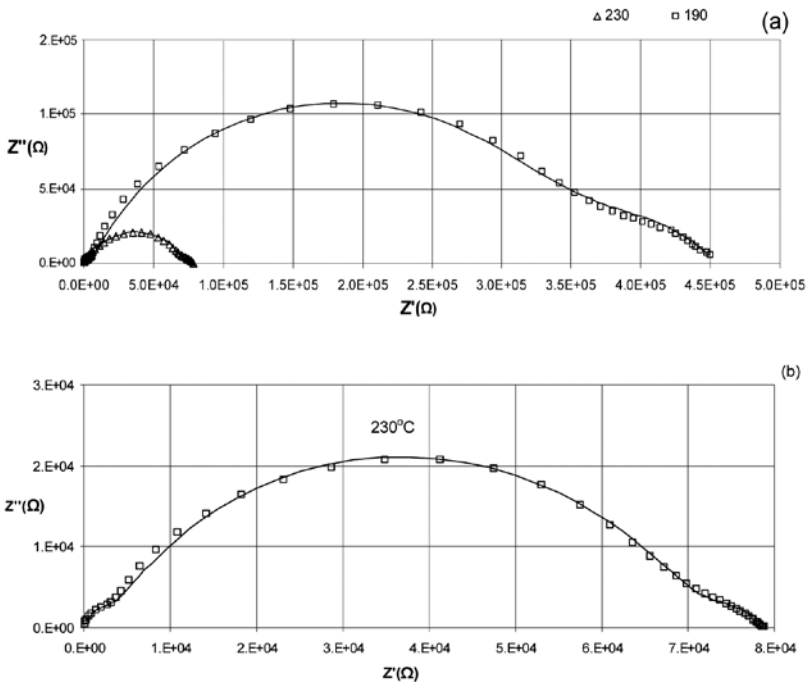


Fig. 3: (a) Complex impedance plots of CSCTO ceramics, with equivalent circuit modelling, at selected temperatures of 190 °C and 230 °C; (b) Complex impedance plots of the CSCTO ceramics, with equivalent circuit modelling at 230 °C

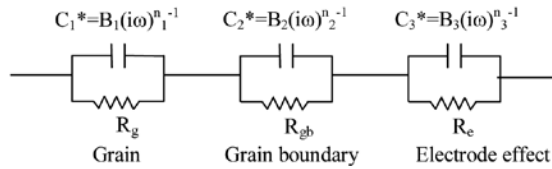


Fig. 4: The equivalent circuit used to model the CSCTO response

Fig. 5 shows the conductivity of the grain and grain boundary of the samples against the reciprocal temperature. The activation energy, E_a values for the CSCTO were 0.31 eV and 0.73 eV for the grain and grain boundary conductivity, respectively. The activation energy value of the grain is smaller than the grain boundary because of its characteristic, i.e. the grain possesses a semi-conducting behaviour, which is more conducting than the grain boundary; the grain boundary is insulating, or known also as an internal barrier layer capacitor (IBLC) which needs much lower energy to stimulate the charge carrier by thermal activation (Sinclair *et al.*, 2002).

TABLE 1
The list of fitting parameters for grain, grain boundary and electrode effects for CSCTO at 70 °C, 110 °C, 150 °C, 190 °C and 230 °C

Temperature oC	Universal Capacitor			Resistance
Grain	$B_1(\Omega\text{Hz})^{-1}$	n_1	ω_p (Hz)	R_g (Ω)
70°C	1.81×10^{-10}	1.00	20000	44000
110°C	6.63×10^{-11}	1.00	120000	20000
150°C	9.95×10^{-11}	1.00	200000	8000
190°C	1.18×10^{-10}	1.00	320000	4200
230°C	1.72×10^{-10}	0.98	500000	2500
Grain Boundary	$B_2(\Omega\text{Hz})^{-1}$	n_2	ω_p (Hz)	R_{gb} (Ω)
70°C	3.68×10^{-9}	0.80	0.4	130000000
110°C	6.99×10^{-9}	0.67	4	16500000
150°C	1.95×10^{-8}	0.64	20	2320000
190°C	1.76×10^{-8}	0.70	250	330000
230°C	1.99×10^{-8}	0.70	2000	68000
Electrode Effect	$B_3(\Omega\text{Hz})^{-1}$	n_3	ω_p (Hz)	R_e (Ω)
70°C	8.07×10^{-8}	0.80	0.02	82000000
110°C	2.99×10^{-7}	0.60	0.03	9100000
150°C	1.89×10^{-6}	0.58	0.07	850000
190°C	2.29×10^{-6}	0.51	2	120000
230°C	1.71×10^{-5}	0.55	5	8800

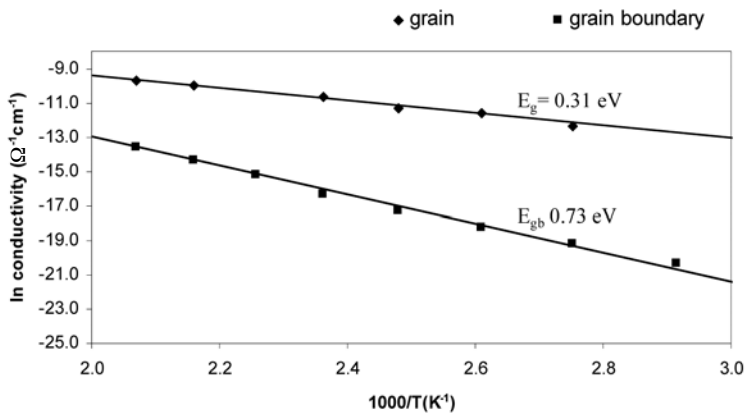


Fig. 5: The Arrhenius plots of (a) the grain conductivity, and (b) grain boundary conductivity of the CSCTO ceramic sintered at 1050°C

CONCLUSIONS

The XRD patterns for the CSCTO show a single phase with a cubic structure. The dielectric response of the polycrystalline CSCTO yielded three semi-circles and are modelled by a series combination of three parallel RC circuits representing grain, grain boundary and electrode effect response. The activation energy, E_a value for the CSCTO is 0.31 eV and 0.73 eV for grain and grain boundary regions, respectively.

ACKNOWLEDGEMENTS

The authors gratefully acknowledge the research grant given by the Ministry of Science, Technology and Innovation, Malaysia (MOSTI), under the Fundamental Research vote no. (5523122) and the Department of Physics, Universiti Putra Malaysia.

REFERENCES

- BOCHU, B., DESCHIZEAUX, M.N., JOUBERT, J.C., COLLOMB, A., CHENAVAS, J. and MAREZIO, M. (1979). Synthese et caraterisation d'une serie de titanates perowskites isotopes de $[\text{CaCu}_3](\text{Mn}_4)\text{O}_{12}$. *J. Solid State Chem*, 29, 291-298.
- OHWA, H., IWATA, M. and ISHIBASHI, Y. (2004). Dielectric properties in $\text{ACu}_3\text{Ti}_4\text{O}_{12}$ (A = Ca, Sr, Ba). *Ferroelectrics*, 301, 185-189.
- SUBRAMANIAN, M.A., LI, D. and DUAN, N. (2000). High dielectric constant in $\text{ACu}_3\text{Ti}_4\text{O}_{12}$ and $\text{ACu}_3\text{Ti}_4\text{Fe}_{12}$ phases, *J. Sol. St. Chem.* 151, 323-325.
- JHA, P. ARORA, P. and GANGULI, A.K. (2003). Polymeric citrate precursor route to the synthesis of the high dielectric constant oxide, $\text{CaCu}_3\text{Ti}_4\text{O}_{12}$. *Materials Letters*, 57(16-17), 2443 - 2446.
- GUILLEMET-FRITSCH, S., LEBEY, T., BOULOS, M. and DURAND, B. (2006). Dielectric properties of $\text{CaCu}_3\text{Ti}_4\text{O}_{12}$ based multiphase ceramics. *Journal of the European Ceramic Society*, 26(7), 1245-1257.
- SINCLAIR, D.C., ADAMS, T.B., MORRISON, F.D. and WEST, A.R. (2002). $\text{CaCu}_3\text{Ti}_4\text{O}_{12}$: One-step internal barrier layer capacitor. *Applied Physics Letters*, 80(12), 2153.